

Article

Tyrosinase/Chitosan/Reduced Graphene Oxide Modified Screen-Printed Carbon Electrode for Sensitive and Interference-Free Detection of Dopamine

Cheng-You Liu ¹, Yi-Chieh Chou ¹, Jui-Hsuan Tsai ^{2,3}, Tzu-Ming Huang ^{2,3}, Jian-Zhang Chen ^{2,3,*}  and Yi-Chun Yeh ^{1,*}

¹ Department of Chemistry, National Taiwan Normal University, Taipei 116, Taiwan; liuorange821028@gmail.com (C.-Y.L.); yichieh840730@gmail.com (Y.-C.C.)

² Graduate Institute of Applied Mechanics, National Taiwan University, Taipei 106, Taiwan; R05543013@ntu.edu.tw (J.-H.T.); r06543009@ntu.edu.tw (T.-M.H.)

³ Advanced Research Center for Green Materials Science and Technology, National Taiwan University, Taipei 106, Taiwan

* Correspondence: jchen@ntu.edu.tw (J.-Z.C.); yichuny@ntnu.edu.tw (Y.-C.Y.)

Received: 17 January 2019; Accepted: 6 February 2019; Published: 13 February 2019



Featured Application: This biosensor was used for the detection of dopamine without interference from high concentrations (0.5 mM) of ascorbic acid. In addition, the electrode developed in this study presented a great sensitivity (22 nM) and a broad linear range compared with existing electrochemical sensors in the detection of dopamine. Moreover, the analysis of dopamine in physiological samples was examined.

Abstract: Tyrosinase, chitosan, and reduced graphene oxide (rGO) are sequentially used to modify a screen-printed carbon electrode (SPCE) for the detection of dopamine (DA), without interference from uric acid (UA) or ascorbic acid (AA). The use of tyrosinase significantly improves the detection's specificity. Cyclic voltammetry (CV) measurements demonstrate the high sensitivity and selectivity of the proposed electrochemical sensors, with detection limits of 22 nM and broad linear ranges of 0.4–8 μ M and 40–500 μ M. The fabricated tyrosinase/chitosan/rGO/SPCE electrodes achieve satisfactory results when applied to human urine samples, thereby demonstrating their feasibility for analyzing DA in physiological samples.

Keywords: screen printing; electrochemical biosensor; tyrosinase; chitosan; dopamine; reduced graphene oxide

1. Introduction

Dopamine (DA), a catecholamine neurotransmitter, appears to play a central regulatory role in olfaction, retinal processes, hormonal regulation, cardiovascular processes, and cognitive functions [1,2]. DA is an electroactive compound, and therefore, studies have investigated the use of electrochemical analysis for its detection. However, DA often coexists with ascorbic acid (AA) in biological fluids such as serum and urine [3], both of which oxidize at similar potentials when using conventional electrodes such as glassy carbon electrode (GCE) [4–8], Au [9–15], and Pt [16,17]. To overcome this problem, we developed a simple and quick electrochemical method for the selective determination of DA, with high sensitivity in the presence of AA for diagnostic applications [18–20].

Screen-printing [21–23] is a simple, robust, and cost-effective technology for the mass-production of sensing electrodes. Screen-printed electrodes can be easily modified to enhance their specificity

and sensitivity by introducing DNA, enzymes, or antibodies [21,24]. Enzyme-based electrochemical biosensors integrate a biorecognition enzyme and a mediator on the electrode's surface [25–29]. Furthermore, numerous protein immobilization techniques such as adsorption [30,31], entrapment [32], and cross-linking [33] have been developed. Unfortunately, covalent enzyme cross-linking can interfere with the enzyme's activity owing to the disturbance of the enzymes' native structure. Entrapping enzymes within a matrix including gels, polymers, or inks is one approach for immobilization that does not compromise stability and biological activity. Chitosan, a natural biopolymer, is commonly used for enzyme immobilization, and shows excellent film-forming ability and biocompatibility [34,35]. Furthermore, chitosan-reduced graphene oxide (rGO) nanocomposites have proven to be highly effective in enhancing mechanical and electric properties [36–39], offering better mechanical and electrical stability. Chitosan covalently bound to graphene enhances the oxidation potential and peak current in DA and AA detection due to higher amide functionalization [40]. It has been shown that pi–pi stacking between DA and graphene enhances the sensitivity for DA detection [41]. rGOs have been widely explored in conjugation with various types of biomolecules such as antibodies, and enzymes. The carboxyl functional groups in rGOs are used for higher loading of biomolecules, because of their strong bonding with aminated groups, enzymes, and polymers [26,42]. Tyrosinase, an oxidase, catalyzes the oxidation of tyrosine. Enzyme electrodes provide great biorecognition with narrow substrate specificity. Previously, mechanisms for DA enzyme-based electroanalysis might have been through O₂ reduction catalyzed by tyrosinase and mediated by DA [43]. In the current study, a tyrosinase/chitosan/rGO modified screen-printed carbon electrode (SPCE) was developed for the sensitive and selective detection of DA.

2. Materials and Methods

2.1. Reagents and Chemicals

RGO nanoplatelets (purity: 99%, thickness: <5 nm, sheet diameter: 0.1–5 μm, Golden Innovation Business Co., Ltd. New Taipei City, Taiwan), acetic acid (purity >95%, analytical reagent grade, Fisher Chemical, Fair Lawn, NJ, USA), carbon pastes (C2030519P4, Carbon Graphite Paste, GWENT GROUP, UK), isopropanol (HPLC grade, TEDIA), acetone (HPLC grade, ECHO), OTS (octadecyltrichlorosilane, purity: 95%, ACROS), dodecane (purity: 96%, TEDIA), tyrosinase (Tyr, 2687 U/mg, Sigma-Aldrich, SI-T3824-50KU), sodium chloride (AMRESCO), potassium chloride (Fisher Chemical), sodium phosphate dibasic (Amresco), L(+)-Ascorbic acid (Amresco), 3-hydroxytyramine hydrochloride (purity: 99%, ACROS ORGANICS), 3-(3,4-dihydroxyphenol)-L-alanine (L-DOPA, ACROS ORGANICS), and potassium hexacyanoferrate(III) (ACROS ORGANICS) were used in this study.

2.2. Apparatus

Scanning electron microscopy (SEM, Nova NanoSEM 230, FEI, Hillsboro, OR, USA), contact angle goniometry (model 100SB, Sindatek Instruments Co., Ltd, Taipei city, Taiwan), and attenuated total reflection Fourier transform infrared spectroscopy (ATR-FTIR, NICOLET 6700, Thermo Fisher Scientific, Waltham, MA, USA) were used to characterize electrode materials. DA measurements were performed using an electrochemical workstation (CHI400, CH Instruments, Inc., Austin, TX, USA). Tyrosinase/chitosan/rGO/SPCE was used as a working electrode, and SPCE was used as both reference and counter electrodes. A fresh DA solution was prepared in PBS (0.01 M, pH 7.0) for all measurements.

2.3. Fabrication of the SPCE Electrode

Corning glass substrates were cleaned sequentially by acetone and isopropanol for 15 min. After blow-drying, the glass substrate was immersed in a solution containing 1 mM OTS dodecane solution at room temperature for 15 min. OTS is an amphiphilic reagent that can improve the adhesion between the follow-up screen-printed carbon pastes and the glass substrate. Next, carbon pastes were

screen-printed on the OTS-coated glass substrate, and air-dried at 100 °C to produce a bare SPCE electrode. The electrode configuration is described elsewhere [23]. The SPCE electrodes were stored at room temperature.

2.4. Fabrication of rGO/SPCE Electrode

For fabricating the rGO/SPCE electrode, a 5- μ L mixture solution containing rGO nanoplatelets was drop-casted on the SPCE electrode, and air-dried at 100 °C for 15 min. The rGO nanoplatelet solution was prepared by mixing 10 mg of rGO with 10 mL of 0.1 M acetic acid solution and stirring for one day at room temperature. The rGO/SPCE electrodes were stored at room temperature.

2.5. Fabrication of Chitosan/rGO/SPCE Electrode

For fabricating the chitosan/rGO/SPCE electrode, a 5- μ L mixture solution containing rGO nanoplatelets and chitosan was drop-casted on the SPCE electrode, and air-dried at 60 °C for 15 min. The chitosan/rGO mixture was prepared by mixing 10 mg of rGO and 100 mg of chitosan with 10 mL of 0.1 M acetic acid solution, and stirring overnight at room temperature. The chitosan/rGO/SPCE electrodes were stored at room temperature.

2.6. Fabrication of Tyrosinase/Chitosan/rGO/SPCE

For fabricating the tyrosinase/chitosan/rGO/SPCE electrode, 10 μ L of tyrosinase (2687 U/mL; 1 mg/mL) was prepared in PBS (50 mM, pH 7.0), and drop-casted on the chitosan/rGO/SPCE electrode surface to generate the tyrosinase/chitosan/rGO/SPCE electrode. The tyrosinase/chitosan/rGO/SPCE electrode was incubated at 4 °C overnight, and washed thoroughly with PBS (50 mM, pH 7.0) containing 0.9 wt% NaCl to remove the unbound enzyme. The tyrosinase/chitosan modified electrodes were stored at 4 °C.

2.7. Preparation of Human Urine Samples

Human urine samples were centrifuged at 5000 rpm for 30 min to obtain the supernatants, and then diluted 10-fold with PBS (0.01 M, pH 7.0) before all measurements.

3. Results and Discussion

3.1. Characterizations of Tyrosinase/Chitosan/rGO Biocomposites

3.1.1. Morphology Analysis

SEM was used to inspect the morphologies of four types of sensor electrodes: SPCE, rGO/SPCE, chitosan/rGO/SPCE, and tyrosinase/chitosan/rGO/SPCE (Figure 1). SEM images indicated that rugged surfaces were formed after coating rGOs onto SPCE (Figure 1A,B). Furthermore, the surface of the chitosan and tyrosinase/chitosan modified rGO/SPCE electrodes was smoother and more homogeneous compared to that of the rGO-coated electrodes (Figure 1C,D).

Vibrational spectroscopy was used to verify the immobilization of tyrosinase on chitosan modified electrodes. Figure 2A shows attenuated total reflection fourier-transform infrared spectroscopy (ATR-FTIR) spectra of the chitosan-modified electrode with and without tyrosinase. Chitosan/rGO/SPCE and tyrosinase/chitosan/rGO/SPCE show peaks in the characteristic C=O stretching band of the amide groups at 1643 and 1537 cm^{-1} in the N-H bending of the secondary amide, respectively; these may be due to the hydrogen bonding between chitosan and some residual oxygenated groups in rGO, and electrostatic interaction between positive chitosan charged molecules and anionic species on the rGO surface. In addition, the characteristic absorption curve of tyrosinase/chitosan/rGO/SPCE was close to that of tyrosinase (Figure S1), indicating the existence of tyrosinase on chitosan/rGO.

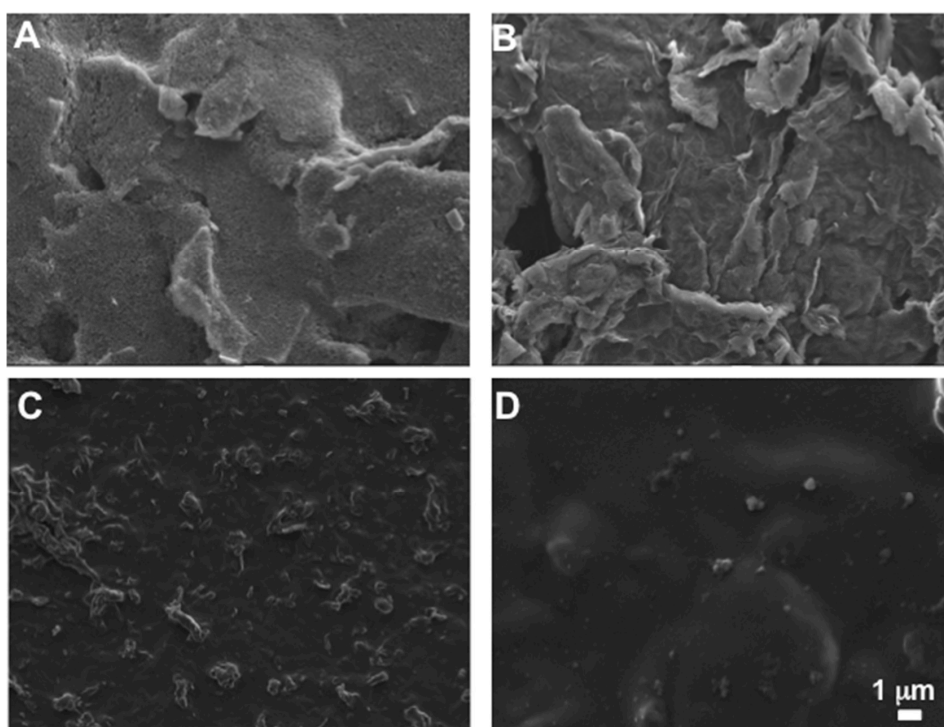


Figure 1. SEM images of: (A) bare screen-printed carbon electrode (SPCE), (B) reduced graphene oxide (rGO) /SPCE, (C) chitosan/rGO/SPCE, and (D) tyrosinase/chitosan/rGO/SPCE.

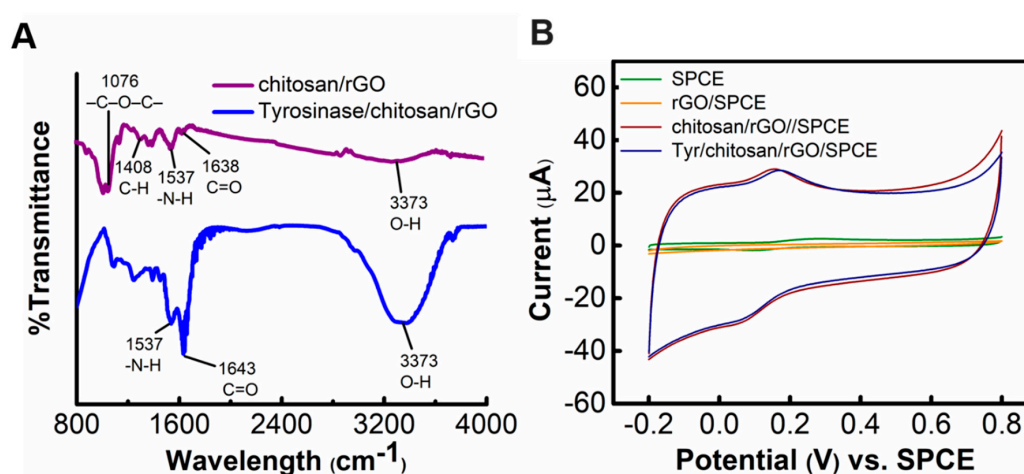


Figure 2. (A) ATR-FTIR spectra of chitosan modified electrode with tyrosinase (blue line) and without tyrosinase (purple line). (B) Cyclic voltammetry (CV) responses (at a scan rate of 100 mVs^{-1}) of the different electrodes in the presence of $10 \mu\text{M}$ of dopamine (DA).

The hydrophilicity of the tyrosinase/chitosan/rGO/SPCE biocomposite electrodes was characterized by measuring the contact angles of a water droplet (Figure S2). Treating rGO with chitosan resulted in a more hydrophilic surface, and the water contact angle changed markedly from 133.80° to 58.55° . However, the contact angle increased to 74.92° after tyrosinase treatment, suggesting successful entrapment of proteins on electrodes.

3.1.2. Cyclic Voltammetry

The four types of electrodes were tested in a solution containing $5 \text{ mM Fe}[\text{CN}_6]^{4-}$ in 0.1 M KCl , at a scan rate of 100 mVs^{-1} . As shown in Figure S3, chitosan/rGO/SPCE and tyrosinase/chitosan/rGO/SPCE had higher oxidation peak current levels compared to those of bare

SPCE, indicating enhanced electroactivity owing to the presence of chitosan. A slight decrease in peak current level was noted after the immobilization of tyrosinase. These findings agree with those obtained in previous studies [26,44].

3.2. Detection of DA

Next, we investigate the CV response of electrodes in DA solutions. Chitosan/rGO/SPCE, and tyrosinase/chitosan/rGO/SPCE showed distinct oxidation peaks at 0.17 V in 10 μM DA solution; the response current levels were also much higher than those of SPCE and rGO/SPCE (Figure 2B). Tyrosinase/chitosan/rGO/SPCE showed similar with a slight decrease in current compared with chitosan/rGO/SPCE, which was attributed to the fact that immobilized enzyme hinders charge transport along the electrode [44]. The influence of pH on the electrochemical response of tyrosinase/chitosan/rGO/SPCEs toward DA was examined. As shown in Figure S4, the peak current level of DA increased with pH, in the pH range of 4.0–7.0, and decreased with a further increase in pH. Therefore, pH of 7.0 was used in the remaining experiments.

As shown in Figure 3A, the peak current intensity increased steadily with DA concentrations; this is attributed to the oxidation of DA to o-quinone by tyrosinase. In addition, the peak current level of DA increased linearly with the logarithmic value of DA concentrations in the range of 0.4–8 μM and 40–500 μM . Figure 3B shows the linear regression equation and correlation coefficient (R^2). The detection limit for DA was calculated at 22 nM based on the signal-to-noise ratio (S/N) = 3. Table S1 compares the linear ranges and limit of detection (LOD) of various carbon-based electrochemical biosensors. The electrode developed in this study shows sensitivity equivalent to, or exceeding, those of existing electrochemical sensors for DA detection. Overall, the sensing electrodes fabricated in this study show a broad linear range and a good detection limit.

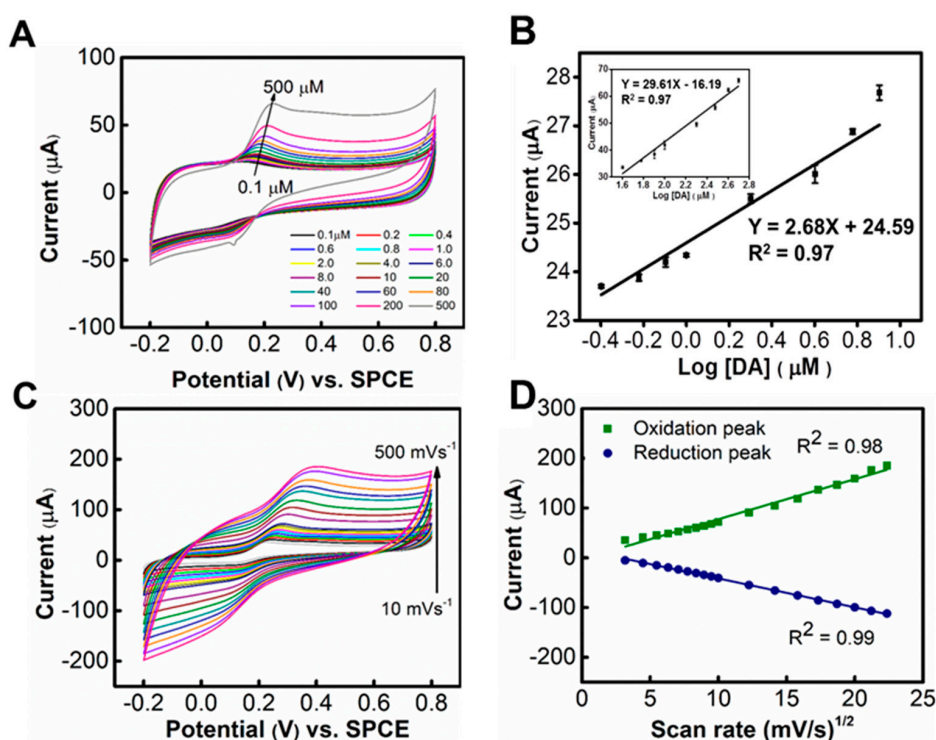


Figure 3. (A) CV curves of tyrosinase/chitosan/rGO/SPCE in the presence of various concentrations of DA (0.1–500 μM). (B) Calibration curve between logarithmic value of DA concentration and oxidation peak currents of the tyrosinase/chitosan/rGO/SPCE. Error bars represent the standard deviation from triplicate measurements. (C) CV of tyrosinase /chitosan/rGO/SPCE at 500 μM of DA with various scan rates (10–500 mVs^{-1}). (D) Calibration curve between square root of scanning rate and oxidation/reduction peak currents.

Figure 3C shows the CV results obtained under various scanning rates (in 500 μM DA, in 0.01 M of PBS at pH 7.0). Increase in both reduction and oxidation peak current levels were observed as the scanning rate increased from 10 to 500 mVs^{-1} . Furthermore, a positive shift in the anodic peak potential and a negative shift in the cathodic peak potential were observed with an increase in the scanning rates. Figure 3D shows a linear relationship between the peak currents and the square root of the scan rate, indicating diffusion-controlled electrochemical kinetics. The diffusion coefficient was calculated to be $4.93 \times 10^{-6} \text{ cm}^2/\text{s}$ (Table S2).

3.3. Interference

Next, we investigated the interference effects of AA and UA. Figure 4A shows CV curves of solutions containing 100 μM of AA, UA, DA, and a mixture of the three. No significant peaks were observed in the presence of AA or UA. Furthermore, the CV curves for DA were nearly identical in the presence and absence of AA. CV curves of chitosan/rGO/SPCE electrodes were examined to verify the role of tyrosinase. As shown in Figure S5, the oxidation peak for detection in the AA solution was significantly higher than that for detection in the DA solution in the presence of AA and DA. The AA concentration in the biospecimen was generally far higher ($\sim 100\text{--}500 \mu\text{M}$) than that of DA; therefore, we increased AA's concentration 10-fold in the presence of various DA concentrations. The peak oxidation current levels in samples with high AA concentrations (500 μM) and DA were nearly identical to those obtained from samples containing DA alone (Figure 4B). We examined the electrodes' stability by measuring the response to 50 μM DA in the presence of 0.5 mM AA. As shown in Figure S6, the peak oxidation current levels obtained from the electrodes were essentially unchanged after being stored at 4 $^\circ\text{C}$ for 28 days.

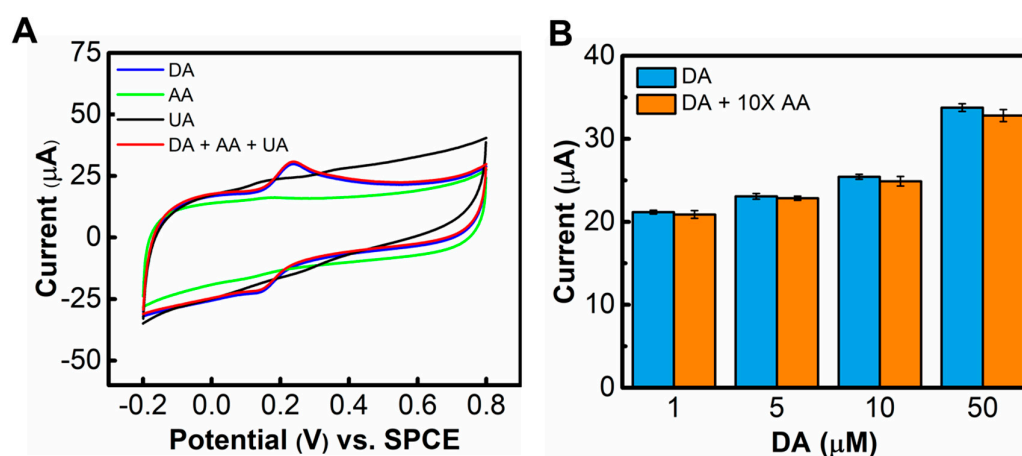


Figure 4. (A) CV curves of tyrosinase/chitosan/rGO/SPCE in the presence of 100 μM AA, UA, DA and the mixture of the three. (B) Peak oxidation current levels of DA in presence/absence of a 10-fold higher concentration of AA. Error bars represent the standard deviation from triplicate measurements.

3.4. Detection of DA in Human Urine

Finally, we evaluated the effectiveness of the electrodes for DA detection in physiological samples. Human urine samples were spiked with various concentrations of DA (Table 1) and then examined using the fabricated tyrosinase/chitosan/rGO/SPCE electrochemical sensor. The oxidation current levels obtained at each concentration via CV were compared with regression results. Table 1 lists the estimated results and the average recovery rates from five measurements. The relative standard deviation (RSD) was larger for urine samples with larger added DA concentrations. The recovery rates were between 93.0% and 97.6%, demonstrating the efficacy of the fabricated tyrosinase/chitosan/rGO/SPCE electrochemical sensor in the detection of DA in real samples.

Table 1. Detection of dopamine (DA) in urine samples (n = 5).

Sample Used	Added (μM)	Found (μM)	RSD (%)	Recovery (%)
Urine sample	8	7.81	0.831	97.6
	2	1.91	0.897	95.7
	0.4	0.37	0.424	93.0

4. Conclusions

In summary, we have developed a tyrosinase/chitosan/rGO/SPCE electrochemical sensor that can quantify DA in the presence of AA and UA. Compared with existing electrochemical biosensors, our device provides satisfactory sensitivity and selectivity toward DA with a wide linear range. Continued investigations using a protein engineering approach can further improve the sensitivity of enzyme-based electrochemical sensing for rapid, selective, and cost-effective DA detection.

Supplementary Materials: The supplementary materials are available online at <http://www.mdpi.com/2076-3417/9/4/622/s1>.

Author Contributions: Methodology, experiments, and data analysis, C.-Y.L., Y.-C.C., J.-H.T., and T.-M.H.; and writing and funding applications, Y.-C.Y. and J.-Z.C.

Funding: This work is funded by the Ministry of Science and Technology of Taiwan under the project number MOST 105-2113-M-003-013-MY2. This work is also financially supported by the “Advanced Research Center for Green Materials Science and Technology” from The Featured Area Research Center Program of the Higher Education Sprout Project by the Ministry of Education (107L9006) and the Ministry of Science and Technology in Taiwan (MOST 106-2221-E-002-193-MY2 & MOST 107-3017-F-002-001).

Conflicts of Interest: The authors declare no conflicts of interest.

References

- Clark, K.L.; Noudoost, B. The role of prefrontal catecholamines in attention and working memory. *Front. Neural Circuits* **2014**, *8*, 1–19. [[CrossRef](#)] [[PubMed](#)]
- Durairaj, S.; Sidhureddy, B.; Cirone, J.; Chen, A.C. Nanomaterials-based electrochemical sensors for in vitro and in vivo analyses of neurotransmitters. *Appl. Sci.* **2018**, *8*, 1504. [[CrossRef](#)]
- O'Neill, R.D. Microvoltammetric techniques and sensors for monitoring neurochemical dynamics in vivo. A review. *Analyst* **1994**, *119*, 767–779. [[CrossRef](#)] [[PubMed](#)]
- Ali, A.; Ensafi, M.T.; Khayamian, T. Simultaneous determination of ascorbic acid, dopamine, and uric acid by differential pulse voltammetry using tiron modified glassy carbon electrode. *Int. J. Electrochem. Sci.* **2010**, *4*, 26895–26901.
- Lin, L.; Chen, J.; Yao, H.; Chen, Y.; Zheng, Y.; Lin, X. Simultaneous determination of dopamine, ascorbic acid and uric acid at poly (evans blue) modified glassy carbon electrode. *Bioelectrochemistry* **2008**, *73*, 11–17. [[CrossRef](#)] [[PubMed](#)]
- Zhang, L. Covalent modification of glassy carbon electrode with cysteine for the determination of dopamine in the presence of ascorbic acid. *Microchim. Acta* **2007**, *161*, 191–200. [[CrossRef](#)]
- Li, Y.; Li, H.; Li, M.; Li, C.; Sun, D.; Yang, B. Porous boron-doped diamond electrode for detection of dopamine and pyridoxine in human serum. *Electrochim. Acta* **2017**, *258*, 744–753. [[CrossRef](#)]
- Dinesh, B.; Saraswathi, R.; Senthil Kumar, A. Water based homogenous carbon ink modified electrode as an efficient sensor system for simultaneous detection of ascorbic acid, dopamine and uric acid. *Electrochim. Acta* **2017**, *233*, 92–104. [[CrossRef](#)]
- Hu, G.Z.; Zhang, D.P.; Wu, W.L.; Yang, Z.S. Selective determination of dopamine in the presence of high concentration of ascorbic acid using nano-au self-assembly glassy carbon electrode. *Colloids Surf. B* **2008**, *62*, 199–205. [[CrossRef](#)]
- Liu, T.; Li, M.; Li, Q. Electroanalysis of dopamine at a gold electrode modified with n-acetylcysteine self-assembled monolayer. *Talanta* **2004**, *63*, 1053–1059. [[CrossRef](#)]
- Oko, D.N.; Garbarino, S.; Zhang, J.; Xu, Z.; Chaker, M.; Ma, D.; Guay, D.; Tavares, A.C. Dopamine and ascorbic acid electro-oxidation on au, aupt and pt nanoparticles prepared by pulse laser ablation in water. *Electrochim. Acta* **2015**, *159*, 174–183. [[CrossRef](#)]

12. Yao, Z.; Yang, X.; Niu, Y.; Wu, F.; Hu, Y.; Yang, Y. Voltammetric dopamine sensor based on a gold electrode modified with reduced graphene oxide and Mn₃O₄ on gold nanoparticles. *Microchim. Acta* **2017**, *184*, 2081–2088. [[CrossRef](#)]
13. Zhou, C.; Li, S.; Zhu, W.; Pang, H.; Ma, H. A sensor of a polyoxometalate and Au–Pd alloy for simultaneously detection of dopamine and ascorbic acid. *Electrochim. Acta* **2013**, *113*, 454–463. [[CrossRef](#)]
14. Pruneanu, S.; Biris, A.R.; Pogacean, F.; Socaci, C.; Coros, M.; Rosu, M.C.; Watanabe, F.; Biris, A.S. The influence of uric and ascorbic acid on the electrochemical detection of dopamine using graphene-modified electrodes. *Electrochim. Acta* **2015**, *154*, 197–204. [[CrossRef](#)]
15. Karuppiah, C.; Palanisamy, S.; Chen, S.-M.; Ramaraj, S.K.; Periakaruppan, P. A novel and sensitive amperometric hydrazine sensor based on gold nanoparticles decorated graphite nanosheets modified screen printed carbon electrode. *Electrochim. Acta* **2014**, *139*, 157–164. [[CrossRef](#)]
16. Yu, H.N.; Pang, Y.C.; Tang, J.Y. Polyaniline nanofiber modified platinum electrode used to determination of dopamine by square wave voltammetry technique. *Int. J. Electrochem. Sci.* **2015**, *10*, 8353–8360.
17. Caetano, F.R.; Gevaerd, A.; Castro, E.G.; Bergamini, M.F.; Zarbin, A.J.G.; Marcolino-Junior, L.H. Electroanalytical application of a screen-printed electrode modified by dodecanethiol-stabilized platinum nanoparticles for dapsone determination. *Electrochim. Acta* **2012**, *66*, 265–270. [[CrossRef](#)]
18. Wu, L.; Feng, L.; Ren, J.; Qu, X. Electrochemical detection of dopamine using porphyrin-functionalized graphene. *Biosens. Bioelectron.* **2012**, *34*, 57–62. [[CrossRef](#)]
19. Zhang, L.; Ning, L.; Li, S.; Pang, H.; Zhang, Z.; Ma, H.; Yan, H. Selective electrochemical detection of dopamine in the presence of uric acid and ascorbic acid based on a composite film modified electrode. *RSC Adv.* **2016**, *6*, 66468–66476. [[CrossRef](#)]
20. Gorle, D.B.; Kulandainathan, M.A. Electrochemical sensing of dopamine at the surface of a dopamine grafted graphene oxide/poly(methylene blue) composite modified electrode. *RSC Adv.* **2016**, *6*, 19982–19991. [[CrossRef](#)]
21. Martin, C.; Grgicak, C. The effect of repeated activation on screen-printed carbon electrode cards. *J. Electrochem. Soc.* **2014**, *61*, 1–8. [[CrossRef](#)]
22. Nagles, E.; García-Beltrán, O.; Calderón, J.A. Evaluation of the usefulness of a novel electrochemical sensor in detecting uric acid and dopamine in the presence of ascorbic acid using a screen-printed carbon electrode modified with single walled carbon nanotubes and ionic liquids. *Electrochim. Acta* **2017**, *258*, 512–523. [[CrossRef](#)]
23. Yang, C.H.; Chen, C.W.; Lin, Y.K.; Yeh, Y.C.; Hsu, C.C.; Fan, Y.J.; Yu, I.S.; Chen, J.Z. Atmospheric-pressure plasma jet processed carbon-based electrochemical sensor integrated with a 3D-printed microfluidic channel. *J. Electrochem. Soc.* **2017**, *164*, B534–B541. [[CrossRef](#)]
24. Du, C.X.; Han, L.; Dong, S.L.; Li, L.H.; Wei, Y. A novel procedure for fabricating flexible screen-printed electrodes with improved electrochemical performance. *Iop Conf. Ser. Mater. Sci. Eng.* **2016**, *137*, 1–7. [[CrossRef](#)]
25. Liu, J.; Wang, X.; Wang, T.; Li, D.; Xi, F.; Wang, J.; Wang, E. Functionalization of monolithic and porous three-dimensional graphene by one-step chitosan electrodeposition for enzymatic biosensor. *ACS Appl. Mater. Interfaces* **2014**, *6*, 19997–20002. [[CrossRef](#)] [[PubMed](#)]
26. Reza, K.K.; Ali, M.A.; Srivastava, S.; Agrawal, V.V.; Biradar, A.M. Tyrosinase conjugated reduced graphene oxide based biointerface for bisphenol a sensor. *Biosens. Bioelectron.* **2015**, *74*, 644–651. [[CrossRef](#)] [[PubMed](#)]
27. Wu, L.; Deng, D.; Jin, J.; Lu, X.; Chen, J. Nanographene-based tyrosinase biosensor for rapid detection of bisphenol a. *Biosens. Bioelectron.* **2012**, *35*, 193–199. [[CrossRef](#)]
28. Dutta, G.; Tan, C.; Siddiqui, S.; Arumugam, P.U. Enabling long term monitoring of dopamine using dimensionally stable ultrananocrystalline diamond microelectrodes. *Mater. Res. Express* **2016**, *3*, 1–8. [[CrossRef](#)]
29. Rani, V.S.V.; Arun, K.; Dhanasekaran, T.; Narayanan, V.; Jesudurai, D. Amperometric nanomolar detection of dopamine using metal free carbon nanotubes synthesized by a simple chemical approach. *Mater. Res. Express* **2018**, *5*, 9.
30. Jesionowski, T.; Zdarta, J.; Krajewska, B. Enzyme immobilization by adsorption: A review. *Adsorption* **2014**, *20*, 801–821. [[CrossRef](#)]
31. Quinson, J.; Hidalgo, R.; Ash, P.A.; Dillon, F.; Grobert, N.; Vincent, K.A. Comparison of carbon materials as electrodes for enzyme electrocatalysis: Hydrogenase as a case study. *Faraday Discuss.* **2014**, *172*, 473–496. [[CrossRef](#)]

32. Alarcon-Angeles, G.; Guix, M.; Silva, W.C.; Ramirez-Silva, M.T.; Palomar-Pardave, M.; Romero-Romo, M.; Merkoci, A. Enzyme entrapment by beta-cyclodextrin electropolymerization onto a carbon nanotubes-modified screen-printed electrode. *Biosens. Bioelectron.* **2010**, *26*, 1768–1773. [[CrossRef](#)] [[PubMed](#)]
33. Zejli, H.; Hidalgo-Hidalgo de Cisneros, J.L.; Naranjo-Rodriguez, I.; Liu, B.; Tamsamani, K.R.; Marty, J.L. Phenol biosensor based on sonogel-carbon transducer with tyrosinase alumina sol-gel immobilization. *Anal. Chim. Acta* **2008**, *612*, 198–203. [[CrossRef](#)] [[PubMed](#)]
34. Dincer, A.; Becerik, S.; Aydemir, T. Immobilization of tyrosinase on chitosan-clay composite beads. *Int. J. Biol. Macromol.* **2012**, *50*, 815–820. [[CrossRef](#)]
35. Ragusa, A.; Priore, P.; Giudetti, A.M.; Ciccarella, G.; Gaballo, A. Neuroprotective investigation of chitosan nanoparticles for dopamine delivery. *Appl. Sci.* **2018**, *8*, 474. [[CrossRef](#)]
36. Justin, R.; Chen, B. Strong and conductive chitosan–reduced graphene oxide nanocomposites for transdermal drug delivery. *J. Mater. Chem. B* **2014**, *2*, 3759–3770. [[CrossRef](#)]
37. Yang, X.; Tu, Y.; Li, L.; Shang, S.; Tao, X.-M. Well-dispersed chitosan/graphene oxide nanocomposites. *ACS Appl. Mater. Interfaces* **2010**, *2*, 1707–1713. [[CrossRef](#)]
38. Zhou, T.; Qi, X.; Bai, H.; Fu, Q. The different effect of reduced graphene oxide and graphene oxide on the performance of chitosan by using homogenous fillers. *RSC Adv.* **2016**, *6*, 34153–34158. [[CrossRef](#)]
39. Liu, B.; Lian, H.T.; Yin, J.F.; Sun, X.Y. Dopamine molecularly imprinted electrochemical sensor based on graphene–chitosan composite. *Electrochim. Acta* **2012**, *75*, 108–114. [[CrossRef](#)]
40. Begum, H.; Ahmed, M.S.; Jeon, S. New approach for porous chitosan-graphene matrix preparation through enhanced amidation for synergic detection of dopamine and uric acid. *ACS Omega* **2017**, *2*, 3043–3054. [[CrossRef](#)]
41. Wang, Y.; Li, Y.; Tang, L.; Lu, J.; Li, J. Application of graphene-modified electrode for selective detection of dopamine. *Electrochem. Commun.* **2009**, *11*, 889–892. [[CrossRef](#)]
42. Parlak, O.; Turner, A.P.; Tiwari, A. On/off-switchable zipper-like bioelectronics on a graphene interface. *Adv. Mater.* **2014**, *26*, 482–486. [[CrossRef](#)] [[PubMed](#)]
43. Ferapontova, E.E. Electrochemical analysis of dopamine: Perspectives of specific in vivo detection. *Electrochim. Acta* **2017**, *245*, 664–671. [[CrossRef](#)]
44. Reza, K.K.; Ali, M.A.; Singh, M.K.; Agrawal, V.V.; Biradar, A.M. Amperometric enzymatic determination of bisphenol a using an ito electrode modified with reduced graphene oxide and mn_3o_4 nanoparticles in a chitosan matrix. *Microchim. Acta* **2017**, *184*, 1809–1816. [[CrossRef](#)]



© 2019 by the authors. Licensee MDPI, Basel, Switzerland. This article is an open access article distributed under the terms and conditions of the Creative Commons Attribution (CC BY) license (<http://creativecommons.org/licenses/by/4.0/>).